Journal of Engineering Research and Reports

13(1): 21-34, 2020; Article no.JERR.57496
ISSN: 2582-2926

Wind Analysis of High-Rise Building Resting on Sloping (Hilly) Grounds of Federal Capital Territory, Abuja, Nigeria

Roy O. Ononye[1*], Kevin C. Okolie[2], F. O. Ezeokoli[2] and S. C. Ugochukwu[3]

[1]Department of Building Technology Education, Federal College of Education (Technical) Asaba, Nigeria.
[2]Department of Building, Nnamdi Azikiwe University, Awka, Nigeria.
[3]Department of Quantity Surveying, Nnamdi Azikiwe University, Awka. Nigeria.

Authors' contributions

This work was carried out in collaboration with all authors. Author KCO designed the study. Author FOE wrote the protocol. Authors ROO and FOE wrote the first draft of the manuscript and managed the analyses of the study and managed the literature searches. Authors KCO, FOE and SCU are supervisors for this manuscript. All authors read and approved the final manuscript.

Article Information

DOI: 10.9734/JERR/2020/v13i117092
Editor(s):
(1) Dr. Guang YihSheu, Chang-Jung Christian University, Taiwan.
Reviewers:
(1) Mustapha Asuku Raji, University of Seoul, South Korea.
(2) Gazali, Sikirulahi Adewole, Nigeria.
Complete Peer review History: http://www.sdiarticle4.com/review-history/57496

Original Research Article

Received 18 March 2020
Accepted 24 May 2020
Published 29 May 2020

ABSTRACT

The importance of wind induced vibration is a key factor in the analysis, design and construction of high-rise building structures. Owing to scarce land resources, urbanization and ever-growing demand for accommodation is leading developers into sloping (hilly) grounds which in turn requires researches on the structural equilibrium of these structures. This study draws to mind the requirements of a fast-growing city of the Federal Capital Territory, FCT, Abuja considering her vast undulating planes and plateaus, high altitudes and windspeeds (50 m/s). Here therein, lies a comparative study of different types of building configurations and responses for sloping grounds using approaches form seismic analyses as a background to achieving set objectives. The study therefore, attempts the application of a commonly used method (Static Wind Analysis, SWA) for analysis of wind loads on structures and also understudying the outcomes of applying the same

**Corresponding author: Email: royrovas@yahoo.com;*

loads using dynamic method (Response Spectrum Analysis, RSA). STAAD Pro V8i software was used to synthesize both analyses using the ASCE 705 code (wind speed-up over Hills) on 40 models for each analysis method for a 3x5 planar building configurations (G+6, G+8, G+12 and G+18) on grounds (0°, 6°, 14°, 18°, and 27°). The findings confirmed the complexities of sloping ground buildings with a greater chance of vibration and sway for SWA than in RSA. It was concluded, that the Stepback-setback (STPB-SETB) frames were better configured to combat wind loads on sloping grounds for both analyses. Recommendations includes, prioritizing the construction industry, collaboration with international bodies on High-rise development, developing a data base and wind testing facilities.

Keywords: Building configurations; high-rise; wind loads; response spectrum analysis; setback; Stepback; Stepback-setback; slope angles; static wind analysis.

1. INTRODUCTION

Wind affects buildings with two distinct effects, buffeting and vertex shedding causing drifts and oscillations [1]. Wind load may be taken as a critical loading, and complicated dynamic wind load in effect controls the architectural/structural design of the structure. Structural Engineers/Construction Technologist are facing the challenges of striving for the most efficient and economical design in high rise building with accuracy in such a way that every component of the building structure must resist two types of loads, i.e. vertical load due to gravity, and lateral load due to earth movements and wind, while ensuring that the final design of the building must be serviceable for its intended use over its design lifespan. Geographical Information Systems (GIS) applications are rudimental in the calculations of different ground slope angles [2] required to establish how wind speed-up hills and the response of bluff bodies along-wind cross section. In understanding the mechanisms of wind-induced static and dynamic loads and reduce the risk of damage, wind tunnel testing has been carried out by many researchers and proven to be an effective tool to investigate wind loads acting on high-rise buildings [3].

Expert assessment on wind engineering have postulated that wind pressures for buildings exceeding 200 m shows can be disastrous on the overall strength of the building than a 9-point earthquake [4]. Wind loads may not necessarily be very high to cause damage. A very good example for modern day wind engineering lesson was the *Tacoma Narrows bridge 1940* which failed under moderate wind speed (68 km/h) due to negative aerodynamic damping or self-excitation [5]. Hilly grounds provide the altitude for an intense wind load on structures as it further compresses its volume towards the peak of the hill, thus increasing its velocity along the slope of the hill. This has necessitated the study of wind applications in high-rise building delivery, considering the irregularities of building configurations and systems for hilly regions observed in the FCT, Abuja and Nigeria.

Researches conducted within the last 2 decades shows that the building responses in the across wind and torsional directions are at least substantial as compared with the response in along wind direction [6]. The along-wind response of a tall building is generally considered by applying the quasi-steady theory [7], which assumes that the fluctuating pressure on the windward face on the structure varies directly with the fluctuation of the longitudinal wind velocity upstream. There are two types of wind directionality factors. One defines a wind directionality factor that changes with direction, as shown in [8,9,10], except for the cyclone-prone regions. The other defines a constant reduction coefficient regardless of wind direction, as in the ASCE 7-98 standard.

The aim of the study is to analyse the structural response and effectiveness of high rise RC buildings frames with different configurations resting on sloping (hilly) grounds of the FCT, Abuja, subjected to prevailing wind load with a view to determine critical response analyses of SWA and RSA, thus prescribing a suitable configuration for high-rise building construction and practice. Results are centred on maximum bending moments, maximum share force, displacement and resultants.

1.1 High-Rise Buildings on Sloping Grounds

According to the Council on Tall Buildings and Urban Habitat, factors that determine a building be classified as a “tall building”, are hinged on displays high-rise qualities of height relative to context, proportions and tall building technologies [11]. From the structural engineer's perspective, a tall building may be defined as one that because of its height, it is affected by lateral forces due to wind and earthquake actions to an extent that they play a critical role in the structural design [12].

A comparative study on the effect of different wind velocity on different sloping ground (0°, 5°, 10°& 15°) using STAAD. Pro software for modelling 2-D frame, observed maximum bending moment in beams for different building heights increases with increase in the wind velocity whereas minute change in moment on beam due to slope moments in column increases with increase in the wind velocity as well as ground slope [13].

A study of twenty-four (24) buildings of G +10, G+15, G+20 of setback, step back with setback on plain ground, sloped ground of 0°, 10°,15°, 20° were analysed using Time history method and response spectrum method with the aid of STAAD Pro. and concluded from analysis, was the performance of set-step back building during seismic excitation as more vulnerable than other building configurations [14].

1.2 Wind Pattern in Nigeria, (Study Region)

Considerable amount of works has been carried out to investigate the characteristics and pattern of wind speed across Nigeria with accessibility to wind speed data information [15,16,17]. All studies draw the same conclusion as to the northern part of the country having highest wind speed. An improvement on the Soboyejo Isopleths [18] and the Nigerian Meteorological Agency (NIMET) wind map with considerations for structural/construction design processes led to the conclusion of subdividing the country into five main categories (Zones) with a yearly mean of 35 to 42 m/s (Category I), 42 to 45.8 m/s (Category II), 45.8 to 50 m/s (Category III), 50 to 55 (Category IV) and 55 to 56m/s (Category V) respectively [19].

The study area, Federal Capital Territory, FCT, Abuja falls within the category III and the upper limits of 50m/s was selected for this study.

Fig. 1. Map of Nigeria showing the FCT, Abuja

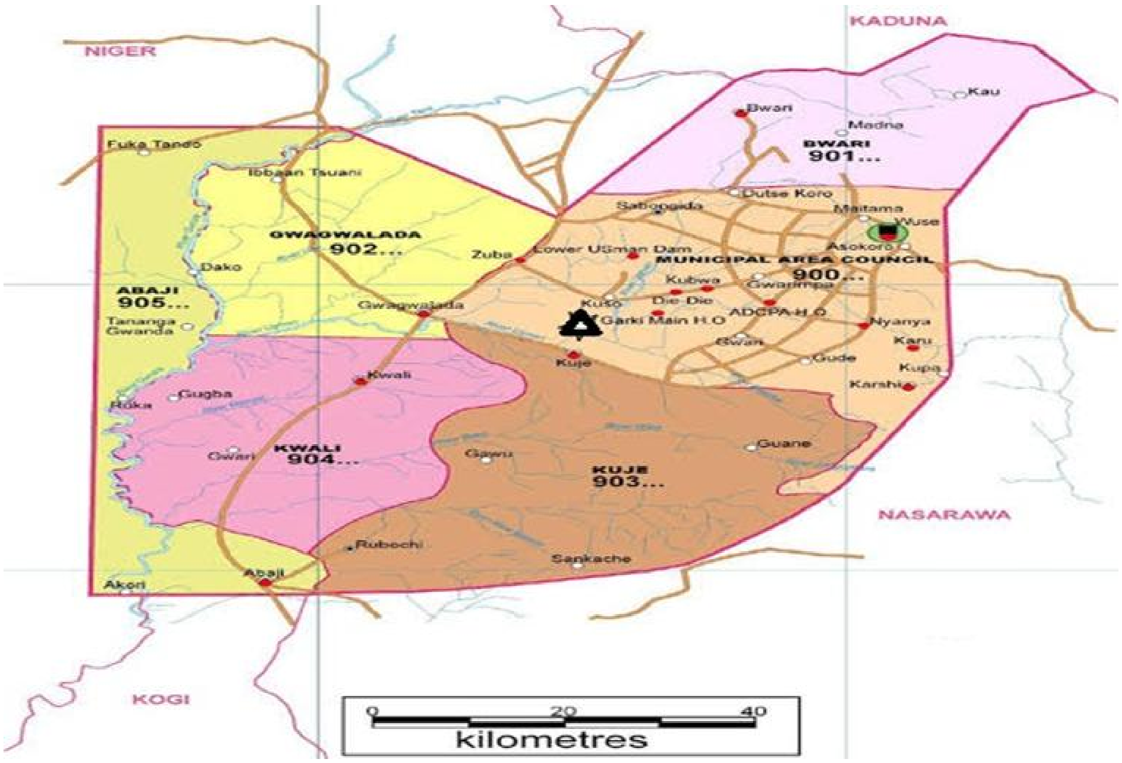

Fig. 2. Map FCT, Abuja showing the Six Area Councils with focus on the Municipal Area Council

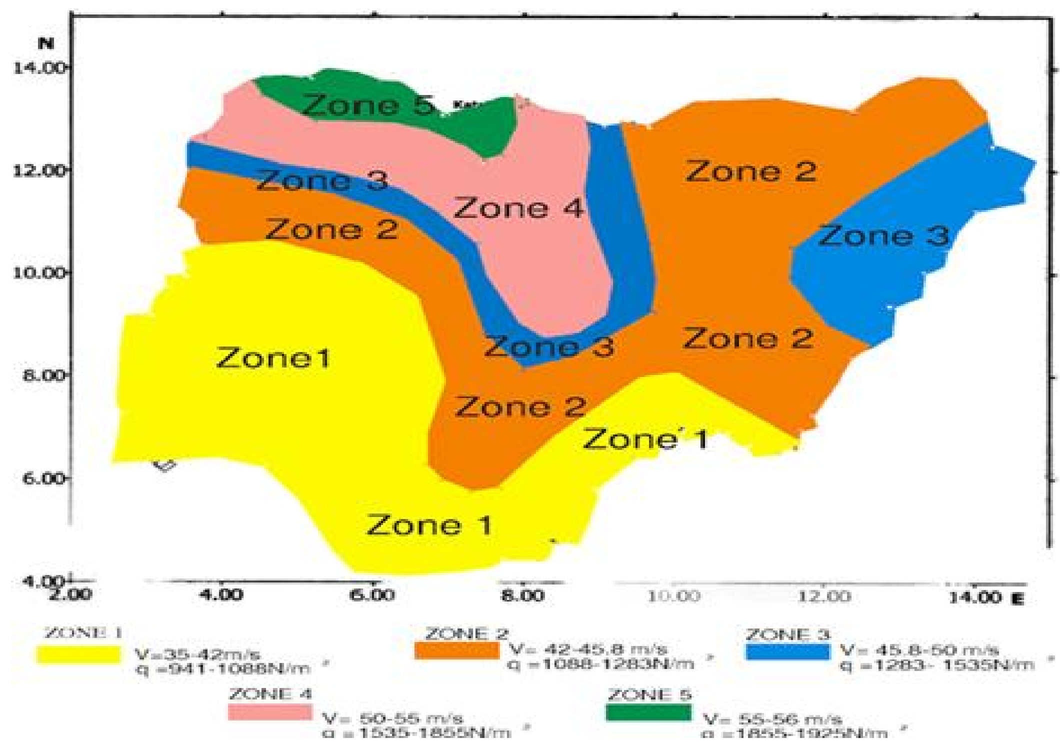

Fig. 3. Classification of Nigeria into Wind Speeds Isopleth Zones [19]

1.3 Code Provisions According to ASCE 7-05

According to chapter 6 of ASCE 7-05, there are three procedures in calculating wind loads for the design of buildings, Main Wind-Force-Resisting Systems (MWFRS), and Components and Cladding viz; Method 1: Simplified Method, Method 2: Analytical Procedure and Method 3: Wind-Tunnel Procedure. The emphasis as regards this study is based on Method 2, which applies to a majority of buildings. The steps of analytical procedure for method 2 are described in ASCE 7 Section 6.5.3 and it's basically built around two fundamental equations, the velocity pressure, q_z equation, and the design wind pressure, p, equation:

$$q_z = 0.613\, K_z K_{zt}\, K_d V^2\, I \text{ (N/m}^2\text{; V in m/s)} \quad (1.1)$$

$$p = qGC_p - qi(GC_{pi}) \text{ (N/m}^2\text{)} \quad (1.2)$$

To determine the design wind load, F, on open buildings and other structure is given by the following formula:

$$F = q_z G C_f A_f \text{ (N)} \quad (2.0)$$

$K_{zt} = (1+K_1K_2K_3)^2$, the multipliers K_1, K_2, K_3 (see Figs. 5-4 Chap.6, ASCE 705)

2. METHODOLOGY

2.1 Problem Formulation

Response Spectrum Analysis (RSA) and Static Wind Analysis (SWA) based on the ASCE 7-05 codebase provisions was performed using Finite Element Analysis model from STAAD Pro V8i software. Various structural outputs such as, base reactions, shear forces, bending moments, displacements/resultants will be computed. The maximum wind speed was adopted from zone 3 (45.8 - 50 m/s) boundary limits and calibrated due to wind speed-up hills effect. A four-group of Reinforced Concrete Building Frames types and configurations were considered, with all having a typical 3x5 bay system having a 9 mX9 m panel, in which first two (set as control reference) are on plane (0°) ground and the remaining two are resting on different degrees of sloping grounds (6°, 14°, 18°, and 27°). The average depth at footing below ground level was taken as 2.5 m where a hard stratum is available. A study of wind induced behaviour of a laterally unsymmetrical high-rise building resting on sloping ground was done considering different structural configurations. Building configurations were specified on basis of the following.

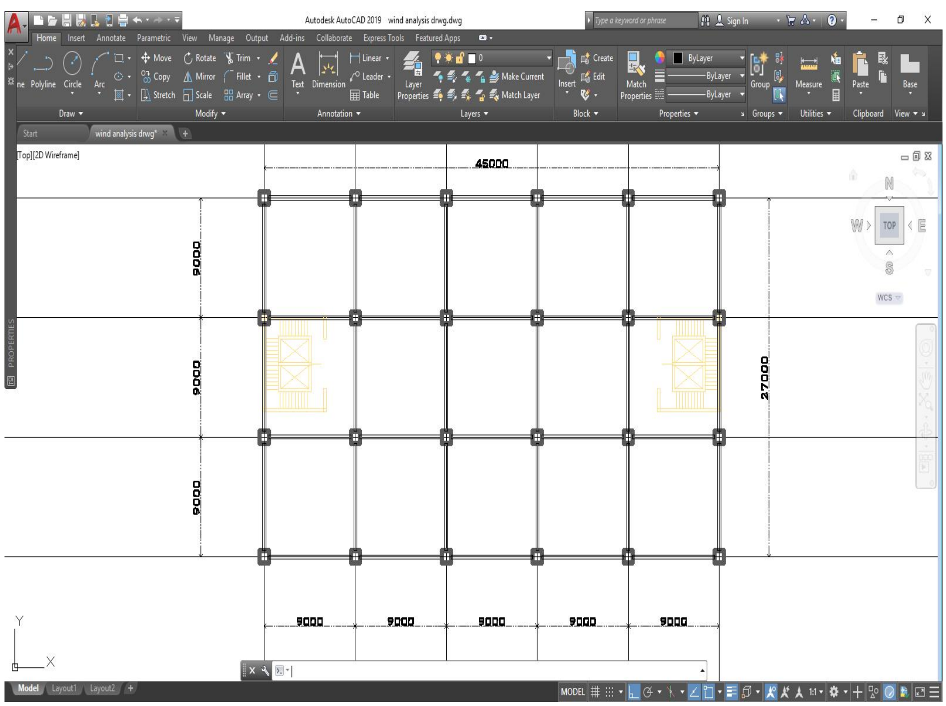

Fig. 4. Plan view of 3x5 bay system with 9 mX9 m planar configuration

2.1.1 Type of frame

Normal Rectangular type of building frame structure (NREC-FRAME): STPB-FRAME (control). Setback type of building frame structure (SETB-FRAME): STPB-SETB-FRAME (control). Step-back type of building frame structure (STPB-FRAME) Step-back Setback type of building frame structure (STPB-SETB-FRAME).

2.1.2 Numbers of storeys

With the study centred on high-rise and its requirements [11], the proposal of between G+6 to G+18 storey R.C building frame was consideration. A ground floor, G, storey height of 5.1 m with subsequent floor storey height of 3.6 m was suggested. Numbers are as follows: G+6=26.7 m; G+8=33.9 m; G+12=48.3 m; and G+18=69.9 m.

2.2 Modelling and Analysis

STAAD Pro. was used for the analyses and pre-programed to adopt the ASCE 7/ACI. To understand the behaviour of each structure, 40 models each were generated for SWA and RSA respectively from AutoCAD software and exported into STAAD Pro V8i, where result verification was facilitated by tools contained in the program's graphical environment.

Table 1. Model/Configuration parametric representation for frame types

Model No.	Configuration		
	Frame type	**Slope angle in °**	**no. of Storeys**
1	NREC	0	G+6
2	NREC	0	G+8
3	NREC	0	G+12
4	NREC	0	G+18
5	SETB	0	G+6
6	SETB	0	G+8
7	SETB	0	G+12
8	SETB	0	G+18
9	STPB 6	5.7 (6)	G+6
10	STPB 14	14	G+6
11	STPB 18	18.4 (18)	G+6
12	STPB 27	26.6 (27)	G+6
13	STPB 6	5.7	G+8
14	STPB 14	14	G+8
15	STPB 18	18.4	G+8
16	STPB 27	26.6	G+8
17	STPB 6	5.7	G+12
18	STPB 14	14	G+12
19	STPB 18	18.4	G+12
20	STPB 27	26.6	G+12
21	STPB 6	5.7	G+18
22	STPB 14	14	G+18
23	STPB 18	18.4	G+18
24	STPB 27	26.6	G+18
25	STPB-SETB 6	5.7	G+6
26	STPB-SETB 14	14	G+6
27	STPB-SETB 18	18.4	G+6
28	STPB-SETB 27	26.6	G+6
29	STPB-SETB 6	5.7	G+8
30	STPB-SETB 14	14	G+8
31	STPB-SETB 18	18.4	G+8
32	STPB-SETB 27	26.6	G+8
33	STPB-SETB 6	5.7	G+12
34	STPB-SETB 14	14	G+12
35	STPB-SETB 18	18.4	G+12
36	STPB-SETB 27	26.6	G+12
37	STPB-SETB 6	5.7	G+18
38	STPB-SETB 14	14	G+18
39	STPB-SETB 18	18.4	G+18
40	STPB-SETB	26.6	G+18

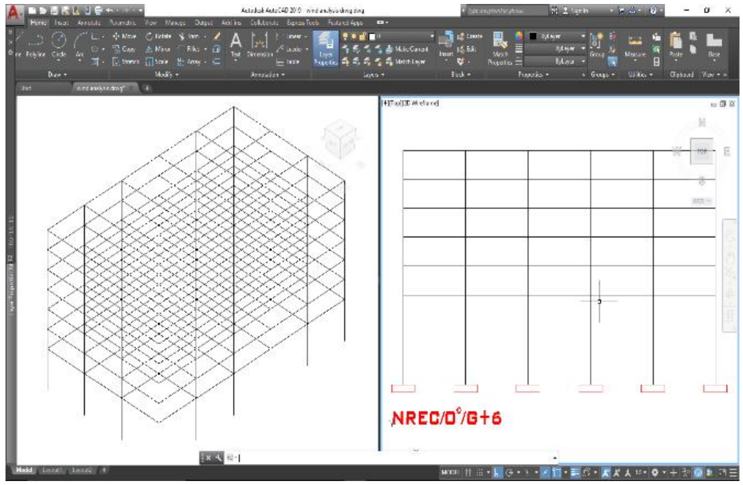

Fig. 4a. 3D/2D view of NERC

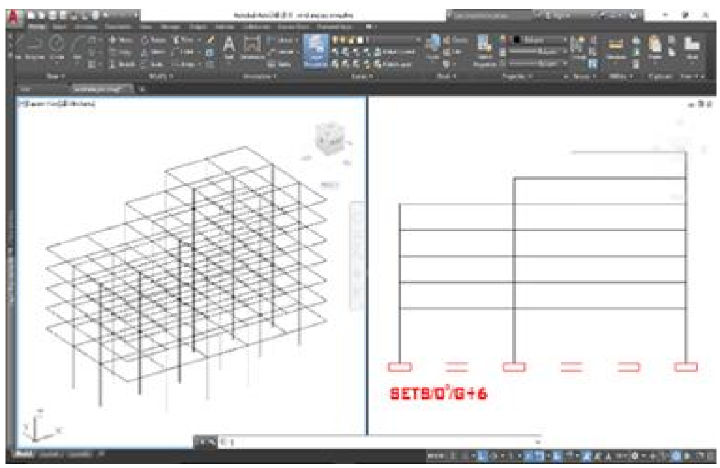

Fig.4b: 3D/2D view of SETB

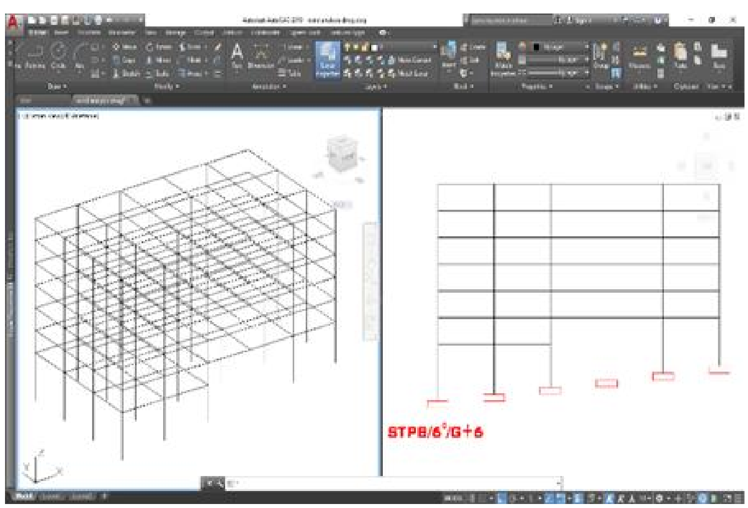

Fig. 4c. 3D/2D view of STPB

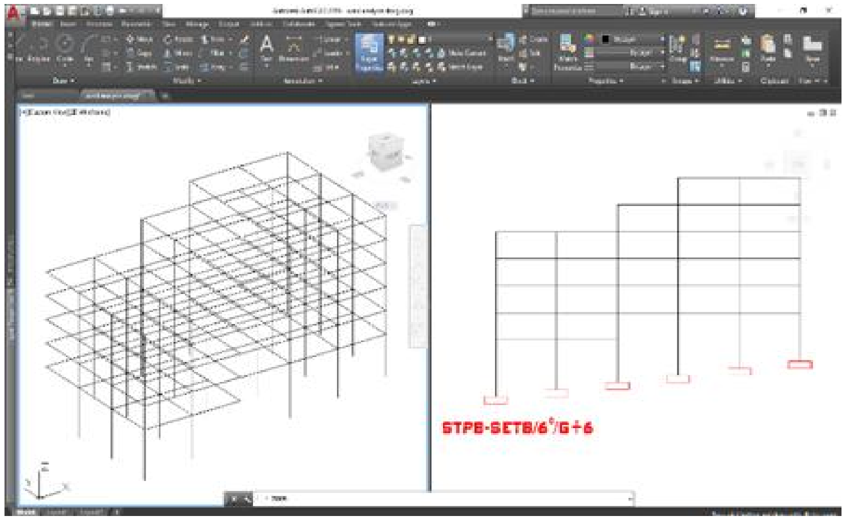

Fig. 4d. 3D/2D view of STPB-SETB

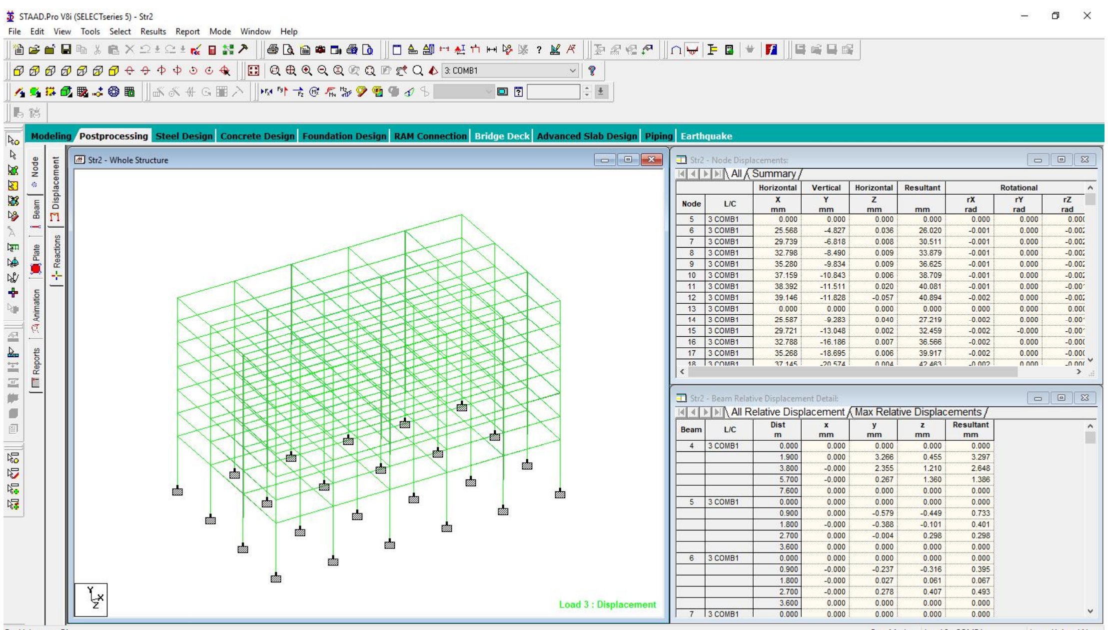

Fig. 5. STAADPro interface

Table 2. Sizes of structural members

S/N	Member	G+6	G+8	G+12	G+18
1	Columns(mm)	450X450	450X450	650X650	650X650
2	Beams(mm)	300X750	300X750	300X750	300X750
3	Slabs(mm)	175	175	175	175

2.2.1 Geometrical/material properties

The approach and accuracy of the analytical results depends on the idealization of the geometry and loading of the structure. The properties required for this study (adopted from ASCE 7-05) were as follows:

2.2.1.1 Loading data

i. Live load: 4.79 KN/m^2 (Table 4-1)
ii. Slab: 4.20 KN/m^2
iii. Floor finish: 1.20 KN/m^2
iv. Partition: 1.00 KN/m^2 (sec.4.2.2)
v. Roof load: 3.02 KN/m^2 (equ.4-2)

vi. Wind load: calculated as per chap.6 ASCE 7-05
vii. Dynamic Pressure coefficient Cp: 3.2 for building category III (Table 5-1)

Loading combination based on occupancy category III

$$1.2D + 1.6W + L + 0.5L_r \quad \text{(sec. 2.3.2)}$$

2.2.1.2 Sizes of members

See Table 2.

2.2.2 Comparative analysis

The analyses were conducted using NREC FRAMES and SETB FRAMES as control configurations to establish a comparative study between STPB FRAMES and STPB-SETB FRAMES on the basis of SWA and RSA.

3. RESULTS AND DISCUSSION

3.1 Results

3.1.1 Results presentation for static wind analysis

See Table 3 - 9.

3.1.2 Results presentation for response spectrum analysis

See Table 10 - 15.

Table 3. Maximum base reactions (KN)

Floors	Frame Types				
	NREC	**STPB 6**	**STPB 14**	**STPB 18**	**STPB 27**
6	10170.229	10031.21	9430.77	9459.133	8755.029
8	15598.854	12552.24	18211.23	13345.29	11470.9
12	19722.42	17893.338	17094.73	19477.64	16926.39
18	25770.574	25417.861	24097.53	24116.95	23278.2
Floors	**Frame Types**				
	SETB	**STPB-SETB 6**	**STPB-SETB 14**	**STPB-SETB 18**	**STPB-SETB 27**
6	10159.12	8640.473	6772.32	6760.046	6065.25
8	12369.397	11347.299	9461.304	9728.317	9791.465
12	17478.803	22057.426	19844.45	18653.9	13168.46
18	24064.912	23003.055	21700.35	20771.08	18198.76

Table 4. Maximum share force in columns (KN)

Floors	Frame Types				
	NREC	**STPB 6**	**STPB 14**	**STPB 18**	**STPB 27**
6	297.501	295.779	292.578	329.622	302.499
8	1335.313	332.922	1358.448	802.568	719.822
12	915.911	473.031	558.436	1329.777	1327.719
18	628.693	682.061	821.093	598.81	844.381
Floors	**Frame Types**				
	SETB	**STPB-SETB 6**	**STPB-SETB 14**	**STPB-SETB 18**	**STPB-SETB 27**
6	707.975	291.462	295.347	299.591	341.052
8	314.351	327.355	294.055	329.946	702.502
12	416.75	1306.907	1304.59	1356.921	990.908
18	627.436	686.199	822.782	606.633	866.753

Table 5. Maximum share force in beams (KN)

Floors	Frame Types				
	NREC	**STPB 6**	**STPB 14**	**STPB 18**	**STPB 27**
6	199.789	190.096	182.917	179.915	172.469
8	287.50	227.829	295.683	251.021	221.988
12	358.641	346.507	332.747	379.483	344.127
18	462.559	453.119	440.655	434.55	417.077
Floors	**Frame Types**				
	SETB	**STPB-SETB 6**	**STPB-SETB 14**	**STPB-SETB 18**	**STPB-SETB 27**
6	215.747	178.594	157.806	152.883	145.308
8	227.62	221.592	187.383	184.31	224.672
12	335.767	257.28	240.199	231.016	207.751
18	424.052	409.426	388.363	377.027	348.482

Table 6. Maximum displacement (mm)

Floors	Frame Types				
	NREC	STPB 6	STPB 14	STPB 18	STPB 27
6	39.146	27.053	74.305	79.3	8.783
8	266.227	154.254	199.799	113.122	118.158
12	211.636	120.98	96.741	145.499	153.389
18	288.106	249.204	207.845	185.676	141.592
Floors	Frame Types				
	SETB	STPB-SETB 6	STPB-SETB 14	STPB-SETB 18	STPB-SETB 27
6	187.597	90.839	75.28	62.721	15.934
8	203.068	214.561	69.376	105.772	104.424
12	149.318	220.698	209.523	165.486	107.791
18	304.532	266.848	226.626	205.33	162.007

Table 7. Maximum bending moments in columns (KN.m)

Floors	Frame Types				
	NREC	STPB 6	STPB 14	STPB 18	STPB 27
6	391.549	373.588	359.851	354.132	339.694
8	566.608	445.793	577.343	491.508	461.799
12	753.339	727.188	698.639	764.804	693.255
18	968.068	948.688	922.822	910.164	873.905
Floors	Frame Types				
	SETB	STPB-SETB 6	STPB-SETB 14	STPB-SETB 18	STPB-SETB 27
6	455.108	353.323	313.124	301.463	287.627
8	447.77	453.497	370.229	362.377	472.654
12	706.661	547.495	508.923	491.172	449.325
18	891.398	860.955	817.113	793.509	734.083

Table 8. Maximum bending moments in beans (KN.m)

Floors	Frame Types				
	NREC	STPB 6	STPB 14	STPB 18	STPB 27
6	591.353	604.709	741.117	803.01	589.342
8	6350.309	993.343	6499.687	2791.342	4200.377
12	2912.772	1736.157	1845.833	5733.456	6787.107
18	2065.686	2537.825	2756.83	2198.801	2966.913
Floors	Frame Types				
	SETB	STPB-SETB 6	STPB-SETB 14	STPB-SETB 18	STPB-SETB 27
6	2354.224	773.71	741.302	708.689	655.027
8	1006.351	1105.115	683.671	842.159	2413.162
12	1414.581	7018.07	7045.419	6876.004	3187.154
18	2068.571	2557.064	2770.928	2384.344	3054.221

Table 9. Maximum resultants (mm)

Floors	Frame Types				
	NREC	STPB 6	STPB 14	STPB 18	STPB 27
6	57.613	47.78	82.45	86.358	30.261
8	786.82	165.191	813.203	259.138	681.124
12	275.244	132.239	109.073	689.041	687.558
18	308.173	270.154	229.509	208.305	167.58
Floors	Frame Types				
	SETB	STPB-SETB 6	STPB-SETB 14	STPB-SETB 18	STPB-SETB 27
6	278.658	95.929	78.14	64.999	19.316
8	211.78	727.183	79.03	111.781	224.761
12	154.84	657.737	654.381	651.545	413.949
18	320.97	282.369	240.483	218.269	173.221

Table 10. Maximum base reactions (KN)

Floors	Frame Types				
	NREC	**STPB 6**	**STPB 14**	**STPB 18**	**STPB 27**
6	9466.581	10382.48	9980.406	9940.492	9193.376
8	15987.24	13026.09	19487.16	14334.5	11879.28
12	20069.18	18337.79	17314.58	19570.78	17307.45
18	26138	26012.84	24570.71	24519.77	23742.09
Floors	**Frame Types**				
	SETB	**STPB-SETB 6**	**STPB-SETB 14**	**STPB-SETB 18**	**STPB-SETB 27**
6	10387.53	9169.742	7359.366	7299.724	6481.919
8	12892.63	11873.79	10183.64	10327.65	10496.86
12	17507.79	22982.65	20860.85	20041.81	14066.19
18	24437.65	23344.76	22165.01	21193.43	18513.21

Table 11. Maximum share forces in columns (KN)

Floors	Frame types				
	NREC	**STPB 6**	**STPB 14**	**STPB 18**	**STPB 27**
6	658.508	1062.947	1180.795	1114.631	4448.13
8	1314.662	1115.267	1429.333	1152.133	1555.356
12	1673.709	1782.739	2416.726	2149.788	3263.074
18	1497.402	1768.727	2461.312	1800.118	2946.418
Floors	**Frame types**				
	SETB	**STPB-SETB 6**	**STPB-SETB 14**	**STPB-SETB 18**	**STPB-SETB 27**
6	711.931	884.959	1044.894	977.785	3362.942
8	772.106	884.027	1156.435	978.408	1854.884
12	1405.195	2503.687	2236.695	1859.599	2856.203
18	1487.125	1619.414	2027.73	1680.319	2599.381

Table 12. Maximum share forces in beams (KN)

Floors	Frame Types				
	NREC	**STPB 6**	**STPB 14**	**STPB 18**	**STPB 27**
6	684.313	932.177	987.615	1112.005	1739.203
8	794.58	1006.956	1041.964	1056.681	1426.138
12	1609.718	1714.282	1658.555	1426.806	1574.012
18	1552.387	1748.368	1687.756	1598.775	2059.516
Floors	**Frame Types**				
	SETB	**STPB-SETB 6**	**STPB-SETB 14**	**STPB-SETB 18**	**STPB-SETB 27**
6	770.935	895.563	889.096	904.921	1294.193
8	866.57	809.514	966.246	906.65	1499.776
12	1545.658	1580.251	1534.599	1419.76	1361.594
18	1628.522	1760.657	1649.582	1643.234	2065.655

Table 13. Maximum bending moments in columns (KN.m)

Floors	Frame Types				
	NREC	**STPB 6**	**STPB 14**	**STPB 18**	**STPB 27**
6	2164.481	2549.479	2525.919	2464.424	2128.108
8	2460.152	2753.121	2347.156	2341.064	1958.325
12	3623.648	3627.255	3437.262	5357.544	4140.753
18	3705.393	3691.119	3491.944	3848.193	3537.479
Floors	**Frame Types**				
	SETB	**STPB-SETB 6**	**STPB-SETB 14**	**STPB-SETB 18**	**STPB-SETB 27**
6	2605.128	2793.323	2274.774	2005.599	1788.173
8	2814.977	2312.643	2517.938	2222.113	2060.487
12	4182.231	3944.118	4786.799	4573.842	3210.776
18	4278.002	4798.971	4793.519	6614.162	5553.071

Table 14. Maximum bending moments in beams (KN.m)

Floors	Frame Types				
	NREC	**STPB 6**	**STPB 14**	**STPB 18**	**STPB 27**
6	2177.915	2740.994	3135.188	2470.173	5122.377
8	6662.771	2884.571	6388.224	3566.538	4216.708
12	4379.744	4560.059	5641.543	7168.077	8717.349
18	3821.391	4498.137	5732.078	7650.722	7820.142
Floors	**Frame Types**				
	SETB	**STPB-SETB 6**	**STPB-SETB 14**	**STPB-SETB 18**	**STPB-SETB 27**
6	2413.924	2510.833	2795.786	2135.653	3827.6
8	2626.775	2010.907	3084.65	2276.9	3168.518
12	3874.554	7612.837	7584.015	7511.045	6900.348
18	3965.101	3958.321	4680.969	6519.134	6883.105

Table 15. Maximum resultants (mm)

Floors	Frame Types				
	NREC	**STPB 6**	**STPB 14**	**STPB 18**	**STPB 27**
6	707.093	771.557	704.509	671.336	379.136
8	3982.794	934.368	2766.449	1536.778	910.954
12	848.525	873.27	868.097	1052.928	1000.643
18	1152.902	2121.281	1254.358	1219.172	1162.328
Floors	**Frame Types**				
	SETB	**STPB-SETB 6**	**STPB-SETB 14**	**STPB-SETB 18**	**STPB-SETB 27**
6	646.123	685.186	502.014	448.69	273.004
8	1013.563	1104.361	651.292	602.067	574.433
12	922.838	914.533	821.643	758.016	1115.839
18	1311.137	1244.039	1156.097	1081.771	927.394

3.2 Discussion

3.2.1 Maximum base reactions

Table 3 and 10 indicates an increase in base reactions with increase in numbers floor relative to frame type and decrease base reactions with increase in slope angle relative to number of floors respectively. In comparation, STPB-SETB frames shows lower base reactions.

3.2.2 Maximum share forces

Table 4 indicates an increase in share forces with increase in slope angle for individual frames with corresponding floors for STPB frames. It was also observed that share forces in STPB frames were lower compared to STPB-SETB frames. Share force in beams (Table 5) increases with increase in number of floors and decreases with increase in slope angle. STPB-SETB frames recorded lower share forces in beams. Table 11 indicates increase in share forces in columns with increase in slope angle for corresponding floors. However, a dip in share force was observed on 12 floors for all slope angles. It was also observed that share forces on STPB frames were higher compared to STPB-SETB frames. Share force in beams (Table 12) indicate increases with increase in number of floors and decreases with increase in slope angle. STPB-SETB frames recorded lower share forces in beams.

3.2.3 Maximum bending moments

Table 7 indicates increase bending moments in columns with increase in number of floors and decreases in bending moments in columns were observed with increase in slope angle. STPB-SETB frames had lower bending moments in columns. However, bending moments in beams (Table 8) showed high level of disparity due to redistribution of moments along increasing slope angles with a dip occurring after the 12 floors for all slope angles. Table 13 indicates increase bending moments in columns with increase in number of floors applicable to STPB-SETB frames, while a dip was recorded at slope angles $18^o/27^o$ on 12 floors for STPB frames. Decreases in bending moments in columns were observed with increase in slope angle with an increase at 18^o for 12 and 18 floors for STPB frames and increase at 18^o for 18 floors for STPB-SETB frames. However, bending moments in beams (Table 14) showed increase in bending moments with increase in number of floors for

STPB/STPB-SETB frames with a dip at 18 floors for all slope angle.

3.2.4 Maximum displacements

Table 6 indicates a decrease in displacement with increase in slope angle and increase in displacement with increase in number of floors. It was also observed that maximum displacements were higher in STPB-SETB frames.

3.2.5 Maximum Resultants

Table 9 indicates increase in resultant with increase in number of floors with a dip at 18 floors for STPB-SETB frames. Increase in resultant with increase in number of floors with a dip occurring between 12 and 18 floors for STPB frames. It was observed that resultant is lower overall in STPB-SETB frames compared to STPB frames at slope angle of 27°. Table 15 indicates a high resultant at 8 floors and a dip at 12 floors followed by a gradual rise. Also, only STPB 27 had a steady increase in resultant, while NREC, STPB 6, STPB 14, and STPB 18 showed similar pattern in resultant computations. It also indicates decrease in resultant with increase in slope angle. SETB and STPB-SETB frames shows similar pattern in resultant computation, while others indicate increase in resultant with increase in number of floors. STPB-SETB frames showed higher resultant.

4. CONCLUSION

The application of two analysis methods used in the comparative study of different configurations of high rise building resting on sloping grounds under the influence of wind loads has led to the conclusion;

Configuration of building frames were not adversely affected by wind load for frames of six and eight floors resting on 6^{o} slope. However, as ground slope increases viz-a-viz number of floors, the Stepback-setback (STPB-SETB) configuration proved effective against wind loads. This was due to the reduction in vertical area and increase in horizontal area of load application. Stepback (STPB) configuration produces more vertical area spaces but will require complicated and advanced system of damping as number of floors increases. It was also concluded, that the windspeed in the study area is not a threat to high rise buildings of up to 18 floors for RSA than in SWA at 12 floors.

Taking a general view of results from analysis of different configuration viz-a-viz ground slopes, their applications in design may reveal complicated processes in construction. Using result from SWA, the introduction of diagonal braces or outriggers technology in combating displacement and sway (torsion) will be a design/construction requirement. Wind pressures influences SWA on all configuration due to noticeable displacement patterns. While, RSA showed negligible displacement owing to the fact that the wind pressure was not enough to trigger excitation, it however revealed high share, which would indicate the introduction of pre/post-tensioned (R.C members) technology in combating the share.

Configuration of building structure is key in presenting a preliminary approach to the challenges of high-rise structure under the action of wind. To this end, some recommendations proffered in this study includes, but not restricted to; engaging researches in high-rise developments through professional workshops, prioritizing the construction industry, collaboration with international bodies on high-rise developments, example is the Council on Tall Buildings and Urban Habitat, CTBUH, and develop a national wind data base and testing facilities that can be readily accessible/assessible in the event of analyses, designs and referencing in all areas of construction.

ACKNOWLEDGEMENTS

The authors are most grateful to the Head of Department of Building, NAU who has been a constant source of guidance and encouragement during this study.

COMPETING INTERESTS

Authors have declared that no competing interests exist.

REFERENCES

1. Kawada T. History of the modern suspension bridge: Solving the dilemma between economy and stiffness. ASCE Press, USA; 2010.
2. Dunn M, Hickey R. The effect of slope algorithms on slope estimates within a GIS. Cartography. 1998;27(1):9–15.
3. Melbourne WH. Comparison of measurements on the CAARC standard tall building model in simulated model wind flows. Journal of Wind Engineering and Industrial Aerodynamics. 1980;6(1):73-88.

4. Vladimir NA, Aleksey AA, Sergey NG, Sergey VK. Numerical simulation of wind loads on high-rise buildings. Proceedings of 13th International Conference on Construction Application of Virtual Reality. London. 2013;620-628.
5. Billah KY, Scanlan RH. Resonance, Tacoma Narrows bridge failure, and undergraduate physics textbooks. Am. J. Phys. 1991;59(2):118-124.
6. Mendis P, Ngo T, Haritos N, Hira A, Samali B, Cheung J. Wind loading on tall buildings. Electronic Journal of Structural Engineering. 2007;7:41-54.
7. Richards P, Hoxey R. Quasi-steady theory and point pressures on a cubic building. Journal of Wind Engineering and Industrial Aerodynamics. 2004;92(14):1173-1190.
8. BS6399-2: British Standard, Loading for Buildings, Part 2. Code of practice for wind loads; 1997.
9. AS/NZS 1170.2: Australian/New Zealand Standard, Structural design actions, Part 2: Wind actions; 2002.
10. Melbourne WH. Designing for directionality, 1st Workshop on Wind Engineering and Industrial Aerodynamics, Highett, Victoria. 1984;1-11.
11. Council on Tall Buildings and Urban Habitat. Criteria for the defining and measuring of tall buildings; 2016. Accessed: 18 November 2017. Available: http:// www.ctbuh.org/resources
12. Stafford SB, Coull A. Tall building structures: Analysis and Design, John Wiley & Sons, New York, N.Y; 1991.
13. Umakant A, Aslam H, Waseem K. Wind analysis of building frames on sloping ground. International Journal of Scientific and Research Publication. 2014;4(5):1-7.
14. Pawar RM. Analysis of set back step-back building resting on sloping ground. Journal of Emerging Technologies and Innovative Research. 2017;4(6):246-253.
15. Medugu DW, Malgwi DI. A Study of wind energy potential: Remedy for fluctuation of electric power in Mubi, Adamawa State, Nigeria. Nigerian Journal of Physics. 2015; 17:40-45.
16. Fadare DA. A statistical analysis of wind energy potential in Ibadan, Nigeria, based on Weibull distribution function. Pacific Journal of Science and Technology. 2008;9:110-119.
17. Fadare DA. The application of artificial neural networks to mapping of wind speed profile for energy application in Nigeria. Applied Energy. 2010;87:934-942.
18. Soboyejo ABO. Distribution of Extreme Winds in Nigeria. The Nigerian Engineer. 1971;7(3):21–34.
19. Onundi LO, Otuagbu P, Oumarou MB. An improvement on the Soboyejo and Nigerian Meteorological Agency Wind Isopleths Maps, Continental Journal of Engineering Sciences. 2009;4:12-19.

Peer-review history:
The peer review history for this paper can be accessed here:
http://www.sdiarticle4.com/review-history/57496